

TIMO: Time Interleaved Multiple Outputs for enabling multiplexing gains with a single RF Chain

Abstract

Massive MIMO is a proponent technology that scales to multiple users using a massive number of antennas. However, an important reason for the lack of deployment of such systems is the complex power-hungry hardware requirement due to a large number of RF chains needed to implement massive MIMO. We present our system Time-Interleaved Multiple Output (TIMO), a novel multi-antenna architecture which achieves Massive MIMO performance by using only a single RF chain. TIMO achieves the above by utilizing RF switches that toggle in sync with a high sampling-rate ADCs, allowing TIMO to capture multiple antenna signals interleaved across time, in essence, virtualizing the concept of a physically laid RF chain. As a consequence of the virtualization of these RF chains to the digital domain, TIMO entails a highly power-efficient, scalable, and flexible multi-user beamforming architecture, which can adapt to the number of users, the channel conditions and provide robust multi-user operation by utilizing scalability in deploying additional antennas for the architecture. We prototype TIMO on a PCB with eight antennas and evaluate it with a WARPv3 SDR platform in an office environment. The results demonstrate that TIMO is 3x more power-efficient than traditional Massive MIMO and 4x more spectrum-efficient than traditional FDMA systems; while multiplexing four users. In this way, our new architecture paves the way for efficient and scalable multi-user communication system.

1 Introduction

The massive adoption of wireless technologies has led to an ever increasing demand for serving more and more devices with never ending throughput demands [1,2]. To meet these demands for each device with scarce spectrum, multi-user MIMO (mu-MIMO) technologies were introduced, which had potential to enable spectrum efficient and concurrent multi-user communications [3,4]. The idea was simply to use the same spectrum to serve K users by utilizing $M = K$ antennas, i.e., create K independent spatial streams, one for each user. However, in practice this $M = K$ MIMO system has failed to consistently deliver multiplicative gains entailed by enabling multi-user transmissions. The core reason has been that often the M antennas have correlated channels for users, i.e. they do not provide independent channels as theoretically conceived, thus making the system of $M = K$ -equations (antennas) and K -variables (user signal) degenerate. In other words, often this system of equations turns out to be non-solvable, or the said wireless channel does not have a full rank.

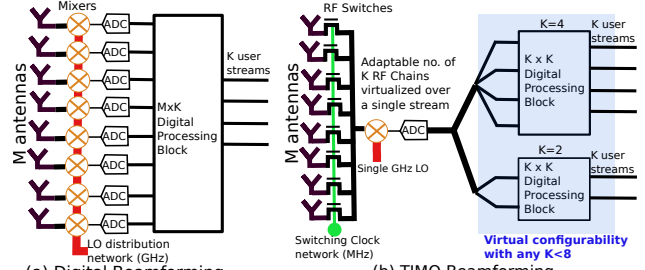


Figure 1: Standard multi-user beamforming arch. vs TIMO

The way to mitigate this problem, and always serve K users robustly, is to sample many more number of equations (more antennas) and have systems where $M \gg K$ antennas to serve K users, referred to as massive MIMO. The challenge with enabling massive MIMO is multiple Radio Frequency (RF) chains and supporting much higher sampling rate and computation thereof. A popular architecture for Massive MIMO utilizes digital beamforming [1, 5], as shown in Fig. 1 (a). Digital beamforming uses separate RF chain per antenna, followed by an ADC sampling. RF chains require an Local Oscillator (LO) at GHz frequencies, which is fed to mixer which downconverts the signal. As a consequence of $M \gg K$, digital beamformers require first, many more RF chains (down-conversion and LO distribution is extremely power hungry) compared to number of users, second requires sampling with many more ADC compared to number of users, and finally, requiring extensive compute to process these samples to only use at a later stage K ADC equivalent samples, making them power-hungry and computationally expensive [6–9]. Furthermore, digital beamformers lacks the flexibility, i.e., when channel is good – one may not need as many antennas – however majority of power is burnt in setting up the RF chains for the antennas.

In stark contrast to the previous Massive MIMO approaches, we present Time Interleaved Multiple Outputs (TIMO), a new class of architecture for base-station/access points that can provide multiplexing gain while *just requiring a single physically laid RF chain* connected to a multi antenna array, thereby saving on energy (shown in Fig. 1b). TIMO achieves this by virtualizing the concept of having physical RF chains per antenna, and instead creates virtual RF chains in digital domain by interleaving samples across time (Fig. 2). This virtualization is made possible by toggling the antennas *on-off* synchronized with receiver’s sampling ADC (Fig. 1(b)), by utilizing RF switches connected to each antenna. RF switches are one of the most readily and lowest-powered hardware component, which helps TIMO create a new immensely powerful architecture, with a single downconversion chain – saving on the ana-

log power consumption. By synchronized toggling of the antennas *on-off* across time with ADC sampling (in MHz), TIMO develops a powerful concept of utilizing time axis to capture the space axis – essentially creating time-interleaved RF chain for capturing all antennas from a single physical RF chain. This allows TIMO to combine digitally amongst these virtual RF chains akin to how a digital beamformer does, albeit with just a single downconversion chain – requiring no LO distribution and multiple mixers operating at GHz frequencies.

Because of the virtualization of physically laid RF chains, TIMO becomes a highly flexible architecture that on one end, can achieve a fully digital beamforming without requiring extensive downconversion chains, and on other end, can flexibly change the sampling rate to adapt the number of virtual RF chains as per demand and thereof computation to save energy. Finally, TIMO can also generalize very easily to a large number of M antennas connected to fewer K virtual RF chains, by mimic analog combining of $M > K$ signals from each of the antennas, to form K output signals summed from different antennas combination, before being sampled in digital domain for virtual RF chain creation. This allows TIMO to achieve networks like hybrid beamformers [10–13] and also avoid issues of hybrid beamformers by flexibly choosing higher sampling rate as necessary for the channel, eliminating fixed K physical RF chains requirement.

In order to implement this combining when $M > K$, TIMO makes a key observation, which is to utilize analog networks where they work the best, viz. increasing of signal power, and digital combiners where they work the best, viz. combining signals with accurate phase and wideband operation to cancel interference. To this end, we present a binarized analog beamforming (BABF) algorithm, which utilizes the constructive combining gains from multiple antennas per virtual RF chain, and thus creates an uncorrelated digital channel which the digital beamformer abstraction then utilizes to kill the interference to almost noise floor (Fig. 7), enabling very robust spectrally efficient multi-user communications.

Thus, to summarize, TIMO designs a new beamforming architecture which utilizes a single wire interface at a higher sample rate to replicate what traditional digital beamformers typically do with multiple wire slower interfaces, at the same time avoiding requirement of multiple downconversion chains. Further, TIMO shows that such architectures are naturally generalizable to a hybrid architectures with more number of antennas than number of RF chains, which allows us to harden the multiplexing gains and thus enable robust mu-MIMO operation. We implement and test our antenna array prototype with WARPv3 SDR and 802.11 OFDM waveforms with 4 users, over multiple user positions in a conference room setting, as well as digital beamforming and FDMA

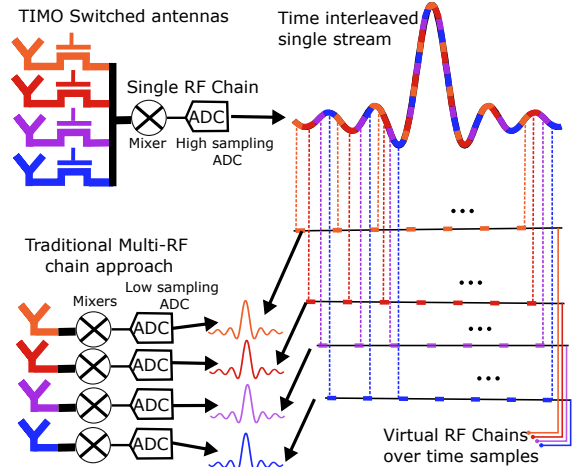


Figure 2: Equivalence of TIMO's virtual RF chains with traditional MIMO's physical RF chains: TIMO uses a single ADC with 4x sampling rate and a network of RF switches that interleave the signal from each antenna over smaller time units. This creates 4 virtual RF chains which can provide the digital samples of 4 antennas equivalent to mu-MIMO system with four physical low-sampling ADCs. (Figure better read in color)

baselines. Our key results include similar performance metrics with digital beamforming with [TODO:4 times] less hardware requirements, achieving the same network capacity as compared to FDMA with 4 times lesser spectrum requirements, and > 10 dB improvement in 90 percentile performance for average SINR across the 4 users by utilizing a hybrid architecture.

2 Related Works

TIMO presents a new spectrum efficient approach to handle multi-users transmissions without utilizing multiple downconversion chains. At the core of our approach lies the creative method of utilizing multiple switched antennas connected to a single high sample rate RF chains to tap into the increased dimensionality from both multiple antennas, and increased sampling rate.

Utilizing more number of antennas than number of RF chains also forms the intended goal of hybrid beamforming architectures being proposed for mmWave communications. Hybrid beamformers have been studied extensively in theory [14–16], system level emulation [12], and extensive hardware implementations [6–8, 10, 11, 13, 17, 18]. The hybrid beamforming architectures can mainly be divided into two categories, fully connected [6–8] and partially connected [10, 17]. In a fully connected architecture, all the antennas are connected to all the RF chains, whereas in partially connected architecture antennas are divided and mapped to different RF chains, hence referred to as partially connected. Fully connected beamformers outperform partially connected, since they capture higher beamforming gains [16], but this comes at a cost of higher hardware complexity [7], and still are limited to narrow band operation as they

use phase-shifter which work optimally for a single frequency instead of wideband. Contrasting to this, utilizing virtual time interleaved RF chains takes away this system complexity and gives us a fully connected architecture by definition, as all the antennas are connected to all the time-slot based RF chains, thus enabling the higher gains without demanding higher hardware complexity, with wide-band operation – as switches are wide-band. Although these traditional hybrid beamformers can realize massive MIMO, they still need more than K RF chains to actually get multiplexing gains, since the multiplexing is enabled by a digital beamforming network for all these architectures.

Previously proposed MIMO interfaces which utilize just a single RF chain [19–21] form the closest of past work related to TIMO. These set of works also utilize a higher IF bandwidth than the users’ transmitted bandwidth. However, instead of combining over time and drawing equivalence to digital beamforming, these works implement analog beamforming and utilize the higher bandwidth only to multiplex the outputs from these analog beamforming blocks. Put more simply, these works either use IF bandwidth code domain [19,20] or different freq. bands in the higher IF bandwidth [21] to multiplex the outputs from a prior analog beamforming front-end. The challenge with these works is that the analog beamforming component also needs to do beam-nulling, which is not very robust to wideband operation and phase shifter inaccuracies [22]. TIMO borrows some of these ideas for channel estimation, where we also use the identity orthogonal codes to facilitate channel estimation, however, the final interference cancellation block in TIMO is fully digital and hence TIMO can do wide-band operation, as well as phase combining with arbitrary accuracy, which makes it stand out of the prior art on single-wire MIMO interfaces.

There are also a parallel set of works which explore switching impedances of a parasitic antenna arrays to create temporal changes in the channel. The first proof of concept demonstration for this technique was in 2010 [23], where a spatial multiplexing parasitic antenna was demonstrated for BPSK signals and 2×2 MIMO scenario. Recently, simulation results have been obtained to extend this beam switching technique to higher modulations like QAM16 [24], as well as OFDM [25–28]. However, there has not yet been an end-to-end OFDM implementation on hardware yet with the parasitic antenna technique. The reasons could be that the technique doesn’t scale well with number of antennas [29], and requires precision control over antenna impedance to generate the required orthogonal beams [28]. Hence, the only implementations for this technique remain to be the first paper in 2010 which used a 3 antenna array [23], and [30] which designed a 4 element array capable of sin-

gle carrier QPSK modulation. Furthermore, the prior effort is leveraging time-diversity to improve the diversity gains or throughput of single user instead of facilitating multi-user. Unlike the past work with these beam switching antennas, TIMO shows that we do not need a specialized antenna array to utilize the said time-diversity benefits, and we can use any commodity antenna with RF switches and make it work with OFDM and higher constellations like QAM-16.

There is also a body of works on Time Modulated Antenna Arrays [31–42]. These works use the same idea of connecting antennas to RF switches, and switch at a faster rate to get diversity gains (SNR improvements). The most notable of these works utilize a 4 antenna array and a 50 MHz switching speed to allow for decoding with a single RF chain [32–34,36,42]. However, this has only been demonstrated for single carrier QPSK constellation for high switching rate of 50 MHz [32], QAM-16, QAM-64 with a lower switching rate of 1 MHz [42], limited to single user. Again, there is no practical implementation extending these ideas to OFDM, and thus to the best of our knowledge, TIMO remains the first practical demonstration of a RF switch based antenna array utilizing high switching rate and OFDM transmissions supporting multi-users and higher order constellations like QAM-16.

There are other papers which target the uplink MIMO problem as well, with some of them requiring coordination from the users to do interference alignment [43,44], set random delays in transmissions to break channel correlations [45], or utilize distributed APs to serve multiple users [46]. Also, there are papers on selecting group of users which can be served efficiently with standard mu-MIMO architectures employing $M = K$, which require a strategic scheduler to manage the multi-user network [47–49]. However, in contrast, TIMO utilizes just a single AP and demands no special coordination from the clients, and hence the clients by default are COTS compliant. Further, we make the multiplexing gains robust for any set of user groupings, by utilizing $M > K$ antennas however still utilizing similar sampling costs.

3 Design

In this section, we present the design of TIMO. First, we describe how TIMO can create numerous virtual RF chains with a single RF chain, saving down-conversion and LO (Local Oscillator) sharing complexity. Next, we discuss how TIMO can achieve flexibility, by showing the analysis that TIMO can behave like both, a true digital beamformer, as well as a hybrid beamformer. Finally, we will discuss an algorithm to make the multiplexing gains from TIMO architecture robust, and conclude by having an overview of our design before moving to the implementation and evaluation of TIMO.

3.1 Creation of time interleaved RF chains with TIMO architecture

TIMO creates virtual RF chains to support multiple user. Let's assume, TIMO attempts to handle K -user by creating K virtual RF chains interleaved across time samples of a single downconverted stream sampled by an ADC sampling K times faster the bandwidth of the users, B_t . In this section, before we generalize to $M > K$ scenario, we would motivate TIMO's design for a simple $M = K$ setting. To further simplify the representations and for brevity we take an example case of $K = 4$.

The intuition behind creation of these $K = 4$ virtual RF chain is that sampling at $4B_t$ to decode B_t bandwidth user, we get 4 extra time slots at our disposal, and for these 4 extra slots we can toggle different antennas on-off using RF switches to capture different antenna's signal in each of the 4 slots. That is, say if we had a bandlimited signal $x[n]$, and we oversample it by 4 times to obtain $y[n]$. To downsample $y[n]$ now, we have 4 possible ways, we can do $y_0[n] = y[4n]$, $y_1[n] = y[4n+1]$, $y_2[n] = y[4n+2]$, $y_3[n] = y[4n+3]$. Each of these y_k 's can be independently used to recover the original signal $x[n]$.

This simple idea of 4 independent ways to downsample $y[n]$ forms the intuitive prior behind TIMO's approach. That is, we can use switch different antennas on for these different sampling instants corresponding to each of the 4 y_k 's and use them as virtual RF chains interleaved over time. The concrete idea here is to keep the first switched antenna to be *on* for 0, 4, 8, ..., $4n$ -th samples, the second switched antenna *on* for 1, 5, 9, ..., $4n+1$ -th samples, and so on. This basically abstracts down to making each y_k as a virtual RF chain for antenna k .

To understand how this virtual RF chain actually captures the wireless channel at k -th antenna, let us model the scenario with $K = 4$ users transmitting signals as $x_i(t)$, $i \in \{1, 2, 3, 4\}$, and the complex time-invariant channel seen by user i to the k -th antenna represented as h_{ik} . We also know that at any time instant, t , each of the RF switch for the k^{th} antenna is either *on* or *off*, which we can model as the switching signal $s_k(t) \in \{0, 1\}$. The combined interference signal $y(t)$ due to the 4 users indexed via i , and 4 switched antennas indexed via k , can be represented as:

$$y(t) = \sum_{i=1}^4 \sum_{k=1}^4 (h_{ik}(t) * x_i(t)) \cdot s_k(t). \quad (1)$$

This combined signal $y(t)$ then goes through one single downconversion, and a single ADC sampling at $4B_t$ to get one single combined digitized signal, $y[n]$ as follows:

$$y[n] \equiv y(nT_s) = \sum_{i=1}^4 \sum_{k=1}^4 (h_{ik}[n] * x_i[n]) \cdot s_k[n]. \quad (2)$$

Now, in order to untangle the individual virtual RF-chain signals $y_k[n]$, $k \in \{1, 2, 3, 4\}$ we need to ensure that only

antenna 1 is *on* for every $4n$ -th sample corresponding to y_0 and *off* for $4n+k$, $k \in \{1, 2, 3\}$ -th samples and so on. We can enable this by choosing the switching vectors $s_k[n]$, $k \in \{1, 2, 3, 4\}$ as $s_1[n] = [1, 0, 0, 0]_n$, $s_2[n] = [0, 1, 0, 0]_n$, $s_3[n] = [0, 0, 1, 0]_n$ and $s_4[n] = [0, 0, 0, 1]_n$, where $[\cdot]_n$ shows that the sequence gets repeated, that is $s_1[n] = 1, 0, 0, 0, 1, 0, 0, 0, \dots$ as shown in Fig. 3. Thus, the oversampled signal $y[n]$ is interleaved with samples from each of the antennas. This forms the core idea behind TIMO's approach of time interleaved RF chains. We can now write these $K = 4$ virtual RF chains, y_1, y_2, y_3, y_4 as

$$\begin{aligned} y_k[n] &= \sum_{i=1}^4 (h_{ik}[4n+k] * x_k[4n+k]) s_k[4n+k] \\ &= \sum_{i=1}^4 (h_{ik}[4n+k] * x_k[4n+k]) \\ &\approx \sum_{i=1}^4 (h_{ik}[4n] * x_k[4n+k]), \end{aligned} \quad (3)$$

where the second step follows from $s_k[4n+k]$ being equal to 1 from definition, and the last step assumes that the wireless channels $h_{ik}[4n] \approx h_{ik}[4n+1] \approx h_{ik}[4n+2] \approx h_{ik}[4n+3]$, which is generally true as the coherence time for channels is usually much larger than duration of 4 samples. Note that we are not assuming that the channel stays same across the entire packet length, but only local stationarity for a 4 sample length.

Thus our k -th virtual RF chain y_k effectively consists of convolution of all the K users signals with channels between the users and the k -th antenna, as only k -th antenna is *on* for the samples used to derive $y_k[n]$ from the single combined stream $y[n]$. This draws a parallel to how in a normal digital beamforming system, we get channels from a RF chain connected to a single antenna. Wherein, we can combine across y_k 's in order to cancel the interference, similar to how digital beamformer utilizes separate spatial RF chains for the same purpose. While, we show only a case for $M = K = 4$ for brevity, the above TIMO's design principles for obtaining virtual RF chains by utilizing switching sequences can be generalized to $M = K$.

3.2 TIMO's equivalence to both digital and hybrid beamforming

In the previous section, we have shown how we can obtain these virtual RF chains y_k by utilizing the switching sequences s_k and using RF switches to implement it with hardware. Before we understand how we perform combining in TIMO, let us generalize the setting to K interfering users and $M > K$ number of antennas. This generalization will concretely reveal how TIMO's single-RF chain architecture can behave as both a digital beamformer, as well as a hybrid beamformer for the traditional multi-RF chain MIMO settings.

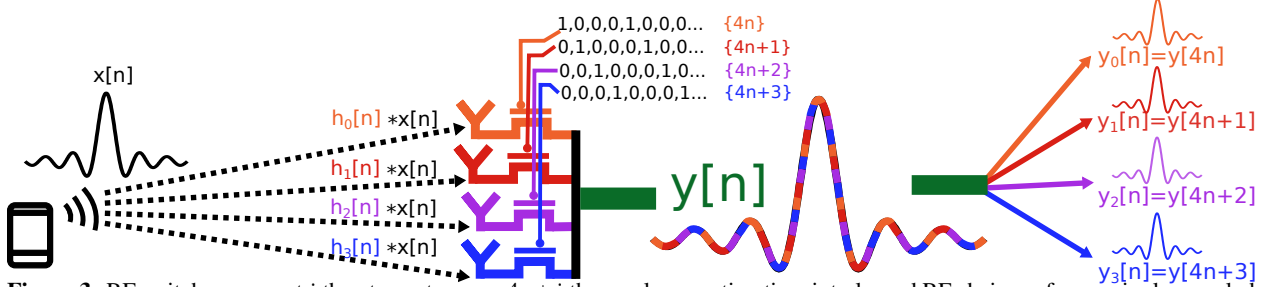


Figure 3: RF switches connect i -th antenna to every $4n + i$ -th samples, creating time interleaved RF chains y_i from a single sampled stream $y[n]$. Thus TIMO obtains multiplexing gains by leveraging the multiple antenna channels across the 4 virtual RF chains.

To understand how the single-RF chain based TIMO's architecture can perform the same as a physically laid multi-RF chain ideal digital or hybrid beamformer, let us first generalize TIMO's combining to $M > K$ setting and understand how TIMO can identify $y_k[n], k = 1, 2, \dots, K$. Firstly, let us stack up the switching sequences as rows of a combined $M \times K$ switching matrix \mathbf{S} . An element $s_{mk} \in \{0, 1\}$ in the matrix \mathbf{S} now represents the on-off states for each of the $m = 1, 2, 3, \dots, M$ antennas for $k = 1, 2, 3, \dots, K$ virtual RF chains. In the example in previous section we had \mathbf{S} as an identity matrix, as only one antenna was *on* at a time. More generally, with i indexing $i = 1, 2, \dots, K$ users, m indexing $1, 2, \dots, M$ antennas and k indexing $1, 2, \dots, K$ virtual RF chains, we can write Eqn (3) as

$$y_k[n] = \sum_{i=1}^K \sum_{m=1}^M (h_{im}[Kn] * x_i[Kn+k]) \cdot s_{mk}, \quad (4)$$

and since s_{mk} can be either 0 or 1 for each antenna m and is independent of the user's transmission we can re-write the above equation as

$$y_k[n] = \sum_{i=1}^K \left(\left(\sum_{m=1}^M h_{im}[Kn] s_{mk} \right) * x_i[Kn+k] \right), \quad (5)$$

Now to make the analysis simpler and to draw easier equivalences with the digital and hybrid beamforming, we can take the Fourier transform to go to the frequency domain as follows:

$$Y_k[f] = \sum_{i=1}^K \left(\left(\sum_{m=1}^M \tilde{H}_{im}[f] s_{mk} \right) \mathcal{F}(x_i[Kn+k]) \right), \quad (6)$$

where $\tilde{H}_{im}[f]$ represents the Fourier transform of channel $\tilde{h}_{im}[n] \approx h_{im}[Kn] \approx h_{im}[Kn+1] \dots \approx h_{im}[Kn+K-1]$, since the channel is assumed to be stationary for every K samples. For brevity, we will drop tilde from the expression and write it simply as $H_{im}[f]$. We can write $\mathcal{F}(x_i[Kn+k]) = e^{j2\pi f k} \mathcal{F}(x_i[Kn]) = e^{j2\pi f k} X_i[f]$ by using Fourier identities for time delayed signals and using the fact that $x_i(t)$ has been oversampled by K times. Thus we get the simplified equation,

$$Y_k[f] = \sum_{i=1}^K \left(\left(\sum_{m=1}^M H_{im}[f] s_{mk} \right) e^{j2\pi f k} X_i[f] \right). \quad (7)$$

Now, note that $\sum_{m=1}^M H_{im}[f] s_{mk}$ is nothing but the (i, k) -th element in the matrix multiplication between $K \times M$

channel matrix $\mathbf{H}[f]$, and the $M \times K$ switching matrix \mathbf{S} . Note that for Y_k we need to remove the phase due to group delay in the Fourier transform, which can be done by multiplying Y_k by $e^{-j2\pi f k}$, and we can write the delay compensated vector $\mathbf{Y}^{\mathcal{D}}[f] = [Y_0[f] Y_1[f] e^{-j2\pi f} \dots Y_{K-1}[f] e^{-j2\pi f (K-1)}]^\top$. This vector $\mathbf{Y}^{\mathcal{D}}[f]$ consists of phase delay compensated Fourier transforms of $y_k[n]$ which were obtained by collecting $Kn+k$ samples in the oversampled signal $y[n]$, and this step is similar to how the popular function `delayseq(.)` [50] removes fractional delays. Denoting $\mathbf{X}[f]$ to be $[X_1[f] X_2[f] \dots X_K[f]]^\top$, to get a much simpler equation in terms of matrix products,

$$\mathbf{Y}^{\mathcal{D}}[f] = (\mathbf{H}[f] \mathbf{S}) \mathbf{X}[f]. \quad (8)$$

This equation is akin to what hybrid analog-digital beamformers use, since \mathbf{S} here is implemented by the analog switching network, and we observe $\mathbf{H}\mathbf{S}$ equivalent $K \times K$ channel with digital streams which can then be combined over digitally.

In digital beamforming systems with $M = K$, we obtain $y_r[n]$ for each of the r -th RF chains, $r = 0, 1, \dots, K-1$, we get the equation

$$\mathbf{Y}^{\text{RF}}[f] = \mathbf{H}[f] \mathbf{X}[f]. \quad (9)$$

For $M = K$ case, we can set the switching matrix \mathbf{S} to be identity, we get a clear equivalence between TIMO and traditional digital beamforming, even though TIMO implements \mathbf{S} in analog domain using switches. However, having $M = K$ is not a very robust operating point to serve K users, since the channel may not always be full rank. Hence, it is always preferred to have $M > K$ in order to serve K users.

Connecting more number of antennas to lesser number of physical RF chains usually requires changing the normal structure of the beamformer and creating specialised analog network with phase shifters. In TIMO's architecture, we have the humble RF switch, which implements this switching network, similar to how setting this network to identity matrix gave TIMO an equivalence to digital beamforming. The main benefit of having $M > K$ antennas for K virtual RF chains is that this allows us to harden the multiplexing gains of K for any user configuration, irrespective of the underlying channels for the K users.

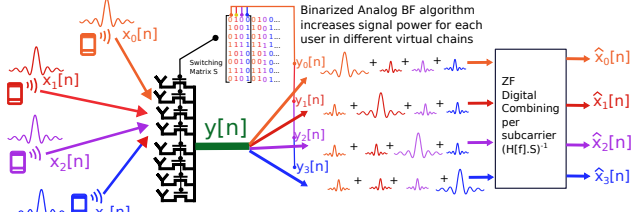


Figure 4: By strategically choosing \mathbf{S} to implement binarized analog beamforming per user, we ensure that the effective $K \times K$ channel is as uncorrelated as possible.

3.3 Harnessing power of multiple antennas for robust multiplexing gains

In previous section, we saw how TIMO provides a much more natural solution to hybridize the digital architecture, by scaling up the number of switched-antennas *without* requiring any additional sampling or downconversion chains cost, or any specialised hardware like phase shifters. In contrast, we have seen that TIMO can easily generalize to $M > K$ antenna scenario and harden the multiplexing gains by $K \times$ with a single RF-chain.

We have seen from Eq 8 that when we have K users and $M > K$ antennas the equivalent channel $\mathbf{H}[f]\mathbf{S}$ still remains $K \times K$, and the digital combining part operates on this $K \times K$ equivalent channel $\mathbf{H}[f]\mathbf{S}$. So the idea here is to choose the matrix \mathbf{S} in a way such that the digital combining operates on a full rank uncorrelated $K \times K$ equivalent channel in order to increase the performance.

In order to achieve this full-rank equivalent channel matrix $\mathbf{H}[f]\mathbf{S}$, we need to choose \mathbf{S} . TO choose \mathbf{S} , we have $2^{M \times K}$ possible choices, as each of the M antenna can be turned on/off for each of the K slots. Hence, a brute force optimization would not be scalable, considering $M = 8$ and $K = 4$, we have 2^{32} choices, and it will take a considerable amount of time to go over these possibilities, which would exceed the channel coherence time. Hence, instead of a brute force search for an optimal \mathbf{S} we need a smart and compute efficient way of estimating a relevant matrix \mathbf{S} .

Here, we make a key observation. We have K users, and the goal is to create equivalent channel $\mathbf{H}[f]\mathbf{S}$ which is as uncorrelated as possible. The way to do this would be to basically use each of the K time slots to prioritize one user at a time, that is, to select column i of \mathbf{S} such that signal power of user i is maximised in that slot. This way the equivalent channel $\mathbf{H}[f]\mathbf{S}$ will have higher diagonal values than non-diagonal, which will decrease correlations, as one user is getting prioritized at a time.

To increase the signal power of user i , the theoretically exact way to do so would be to conjugate the user i 's channels for each antenna, thus implementing analog beamforming, which would co-phase the user's signals received at each antenna, to give constructive combining gains. However, we do not have accurate phase shifters, and infact in our design we just have RF switches which

can toggle on-off, thus providing only one-bit control over the phases. But, at the same time, we just need to increase the signal power for user i and we actually do not need very accurate beamforming for this. This can also be achieved by turning *on* the maximal set of antennas whose phases would add up constructively (Fig. 4). We call this algorithm as binarized analog beamforming (BABF) algorithm, as it takes the analog beamforming solution and finds the closest representative of that in the binary RF switch implementable solution.

To achieve the best uncorrelated equivalent channel matrix $\mathbf{H}[f]\mathbf{S}$, in binarized analog beamforming algorithm, we go one antenna by one to calculate the number of other antennas whose phases lie within an acute angle ($\pi/3$ in our implementation) of each other. We select the group of in-phase antennas having the highest cardinality, since that would entail higher constructive combining gain and thus higher power for user i . Thus, this makes the algorithm to be $O(M)$, as we have to choose from M number of groups. We repeat this procedure for each k -th user for k -th time slot to create a matrix \mathbf{S} that enables maximally uncorrelated equivalent channel matrix. A further detailed implementation of the BABF algorithm is described in Algorithm 1 (in Appendix section).

We note that the BABF method of choosing \mathbf{S} to prioritize signal power instead of utilizing \mathbf{S} to cancel interference is a common theme on how hybrid beamformers [12, 14] choose their analog weights. This is because increasing signal power is an easier operation, and allows for inaccuracies because whatever is in-phase will ultimately add up and serve the purpose of increased signal power. On the other hand choosing an analog network such that signals are cancelled requires more careful calibration, as well as an requirement to generalize to wide-band. Hence, in line with previous approaches to utilize analog networks for creation of such rank achieving equivalent channels, we also propose an algorithm to increase the signal power, however using just RF switches instead of quantized phase shifters. The final task of combining across the signals with arbitrary accuracy and wideband generalization are the tasks of the digital combining part of TIMO which will be described in the next section.

3.4 Final digital combining step in TIMO

The key insight which TIMO delivers is that to handle K users transmitting B_t bandwidth signals \mathbf{X} , we can sample a single signal y at KB_t bandwidth by utilizing a switched antenna array with number of antennas $M > K$ and switching sequences for each of the M antennas and the extra K slots created due to higher sampling rate denoted by \mathbf{S} to get the equation

$$\mathbf{Y}^{\mathcal{D}}[f] = (\mathbf{H}[f]\mathbf{S})\mathbf{X}[f], \quad (10)$$

where $\mathbf{Y}^{\mathcal{D}}$ are the delay compensated K streams derived from y . We get an equivalent channel $\mathbf{H}[f]\mathbf{S}$ created due to the switching network, and we choose \mathbf{S} such that the obtained $K \times K$ channel is as uncorrelated as possible, so that all the K users can be served with sufficient SINR.

Now, to recover individual data symbols for each user $\mathbf{X}[f]$ from the obtained interfered samples $\mathbf{Y}[f]$, we can utilize a $K \times K$ beamforming matrix $\mathbf{V}[f] = [v_1 v_2 \dots v_K]^T$ which is a collection of $K \times 1$ beamforming vectors $v_i, i = 0, 1, \dots, K - 1$. When we take the inner product of v_i with $\mathbf{Y}[f]$, the hope is that we recover $x_i[f]$. To cancel out interference, the best method is to use a ZF combiner [51]. In TIMO's case, the matrix $\mathbf{V}[f]$ selects pseudo inverse of $\mathbf{H}[f]\mathbf{S}$ as the digital combiner matrix \mathbf{V} . Thus after utilizing the digital combiner, we get

$$\mathbf{V}\mathbf{Y}^{\mathcal{D}}[f] = \text{pinv}(\mathbf{H}[f]\mathbf{S})(\mathbf{H}[f]\mathbf{S})\mathbf{X}[f] \approx \mathbf{X}[f], \quad (11)$$

which allows us to remove the interference and recover each of the K symbols $\mathbf{X} = [X_1, X_2, \dots, X_K]^T$. An important point to note is that since this combining happens in digital domain, we can do arbitrary combinations for each frequency bin $[f]$ which allows for resilient wide-band operation, as well as accurate phase values so that the interference are cancelled perfectly.

Extending TIMO to handle downlink multi-user transmissions: So far we have presented analysis of TIMO's beamforming approach applied to an uplink channel with AP receiving multiple-user's interfering signals. In an equivalent downlink setting, almost the same generalization can apply naturally. given the channel measurements at the clients are fed-back to TIMO. TIMO would then utilize the RF switch based architecture to create spatial transmissions which essentially null other users' signals while trying to communicate to an intended user, allowing for downlink multi-user transmissions.

4 Implementation

We implement the TIMO architecture on a custom multi-layer PCB prototype fabricated using Rogers substrate. On the top-layer of the PCB, we design interfaces to utilize COTS antennas via SMA connectors, which are then connected to RF switches, and the output from 8 of these switched antennas is then combined with a wilkinson combiner network matched at the operating frequency for 2.4 GHz. On the bottom layer of the PCB, we have a CMOD-A7 FPGA used to clock the RF switches. The FPGA is connected to a PC via a micro USB cable and allows us to program the RF switches to toggle in different configurations.

We utilize WARPv3 as the SDR for our implementation of an uplink receiver. The sampling clock for WARPv3 is 40 MHz, thus a sampling time period of 25 ns. Coming to the first design principle of TIMO, which is to switch antennas on-off in order to create the time

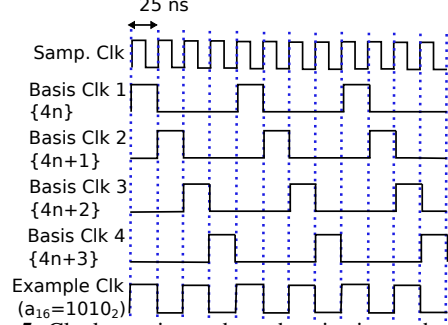


Figure 5: Clock creation and synchronization at the FPGA

interleaved virtual RF chains, we need to switch the antennas on-off in a way that this switching is synchronised with the sampling instants of the SDR. WARPv3 exposes it's sampling clock using the CM-MMCX module, which is then fed to the FPGA, and the FPGA utilizes this sampling clock to then derive the clocking frequencies.

In order to create $K = 4$ virtual RF chains, we would need to switch different antennas on-off for every $\{4n\}$ -th, $\{4n + 1\}$ -th, $\{4n + 2\}$ -th and $\{4n + 3\}$ -th samples. To do so, we create 4 basis clocks in the FPGA, which correspond to these 4 sample groups (Fig. 5). In order to perform channel estimation, we can give these 4 basis clocks to a group of 4 antennas and obtain the corresponding virtual RF chains by collecting these appropriate time samples. This basis clock formulation also allows a scalable way of implementing the switching matrix \mathbf{S} . The switching matrix is a 8×4 matrix, with each i -th row representing the on-off states of the i -th antenna for the 4 different virtual RF chains. For an example, say this row was $[1, 0, 1, 0]$, so this would simply be implemented as $1 * B1 + 0 * B2 + 1 * B3 + 0 * B4$ (Fig. 5), where Bi is the basis clock i .

Thus, in order to implement this matrix in hardware, we represent each row, which is a 4×1 binary vector by a hexadecimal digit, and communicate 8 of these digits to the FPGA via a standard UART code. Then the binary vectors represented by these hexadecimal numbers is multiplied by appropriate basis clocks and the summed clock is then given to each of the 8 antennas. To implement this switching sequence correctly in hardware, we need to select RF switches with tON/tOFF below 25 ns, since otherwise the switches would be too slow to respond to the clocking input. For this we select the commercially available switches HMC197BE [52] which have tRISE = 3 ns, and tON = 10 ns, suitable for our application. These switches have very minimal 0.5 dB insertion loss, and the overall insertion loss from the transmission lines in the PCB amount to about 3 dB. This is 10 dB lower than the current hybrid beamforming approach for sub-6 networks [11].

Since we create $K = 4$ virtual RF chains by our switching, in order to support $K = 4$ users, we fix the bandwidth of transmitters to be 10 MHz. These 10 MHz transmit-

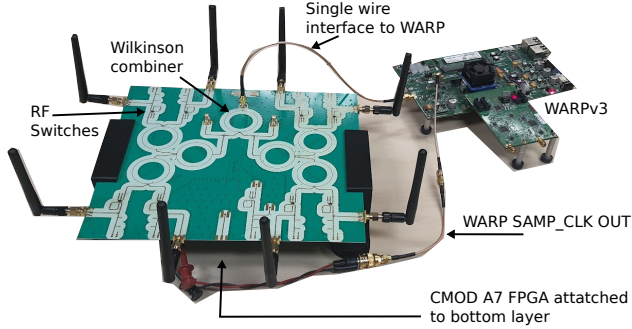


Figure 6: Hardware implementation of TIMO

ters are implemented on different SBX daughterboards using X310 USRP. The transmitting USRPs and the receiving WARP are not synchronized and share a different clock altogether. We have observed that the CFO introduced as a consequence of unsynch TX-RX doesn't play any role in TIMO's performance, as essentially TIMO utilizes a spatial operation, and because of CFO we have some constant phase offsets across the virtual RF chains which are naturally compensated during channel estimation. Note that this choice of transmit bandwidth is constrained because of our choice of receiver SDR, as with WARPv3 we can not do more than 40 MHz sampling (since the MAX2829 IC used in WARP has a maximum RF bandwidth of 40 MHz). Our choice of WARP was also restricted by the requirement of 4 physical RF chains so that we can compare TIMO's approach with 4 physical RF chains. With upcoming SDRs, like X410 [53] having 4 RF chains, and sampling rate well above 100 MHz, we can scale to higher bandwidths in the future.

Finally, to implement the required digital signal processing, we utilize the WARPLab codes in MATLAB to utilize 802.11 compliant OFDM waveform with 64 subcarriers (48 data, 4 pilots and 12 null subcarriers), with the required tweaks to create and utilize these time interleaved RF chains. The channel estimation is done by having the users transmit LTS's separately from each other, and after the last user's LTS is finished the common data transmission mode starts (Fig. 7 (a)). Using the estimated channels from the LTS preamble, the switching matrix \mathbf{S} is calculated via in-phase antenna selection given via Algorithm 1, and to implement this matrix a 8 digit hexadecimal string representing the 8×4 matrix \mathbf{S} is then communicated to the CMOD FPGA via the MATLAB serial library.

As a consequence of utilizing MATLAB, our signal processing toolchain is not real-time and requires post processing of the channel traces obtained by setting the switches under certain configurations. The data processing toolchain is to first utilize identity codes for 4 antennas and zero codes for other 4 antennas, collect received samples from WARP required to estimate these 4 antennas' channels, and then in the next step, do vice

versa, use zero codes for the first 4 antennas and identity codes for next 4. Finally, after we obtain the channel estimates of all the 8 antennas, we calculate the best switching matrix based on Algorithm 1, configure the FPGA via UART communication and then collect the received samples having the equivalent channel of $\mathbf{H}\mathbf{S}$.

For the experiments we set the transmit power such that we have SNR of about 17-20 dB, and utilize QAM-16 constellation with 0.5 rate convolutional channel code. This constellation was tested to work reliably for these SNRs, given the phase noise of our implementation with users on an USRP and AP being WARPv3. We receive this constellation robustly even in presence of 4 user interference, and one of the raw received and processed constellations is shown in Fig. 7 (d), (e).

5 Evaluations

We have evaluated TIMO architecture to deliver uplink mu-MIMO multiplexing gains with just a single RF chain connected to multiple switched antennas. The core principle behind TIMO is the usage of strategic toggling sequences for the RF switches, which enable the creation of time interleaved virtual RF chains. TIMO would then combine across these virtual RF chains in digital domain to cancel interference and thus serve multiple users with a single RF chain. Thus TIMO can be very helpful in situations where the networks need to serve multiple users simultaneously, for example during conferences when the occupancy shoots up drastically.

Hence, we evaluate the performance of TIMO in a conference room setting (Fig. 8a). Evaluation in such conference room, or auditorium settings has been a constant feature of research works on multi-user communications [11, 45]. The room which we choose has rough dimensions of 12m*5m, and is populated with objects like tables, chairs, whiteboard and TV screens, which make the setting rich with scattering effects. Further, we test extensively by placing the transmitters at various locations in the room (Fig. 8b) to capture the overall performance of TIMO in the experimental setting considered.

Comparison with digital beamforming: In our first evaluation experiment, we verify our design principle of the creation of virtual RF chains by creating a faithful test setup to compare virtual RF chains with physical RF chains (Fig. 8c). In this setup, we use RF switches external to the switches we use for our switched antennas, and the purpose of these SPDT RF switches is to toggle between two states. The first state of the setup is "RFC-RF1", which connects the 4 antenna array to the PCB which implements TIMO architecture, and takes the output emanating from the PCB and feeds it to a single RF chain on WARP. The other state, "RFC-RF2" connects the same antenna array to each of the RF chains on WARP to implement digital beamforming. This allows

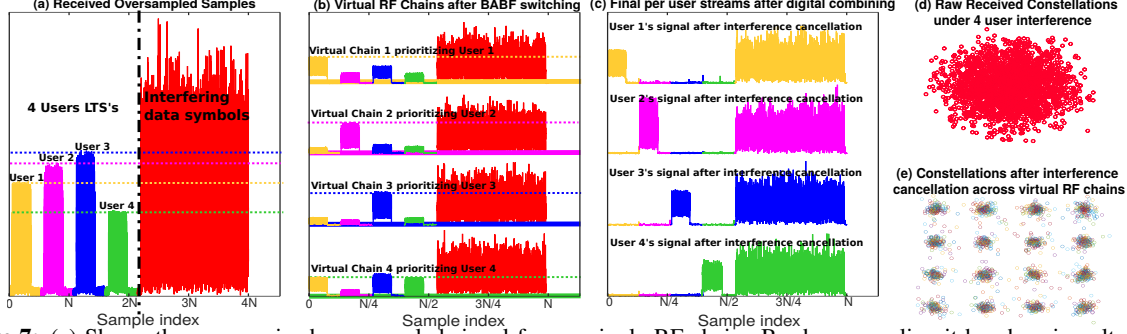


Figure 7: (a) Shows the raw received oversampled signal from a single RF chain. By downsampling it by choosing alternate 4 samples we form the virtual RF chains as shown in (b). (b) depicts the signals after they go through the BABF algorithm which increases user i 's power in i -th virtual chain. Finally (c) shows the interference free per-user streams obtained after digital combining of the virtual chains in (b). We also show the raw constellations before (d) and after (e) the interference cancellation.

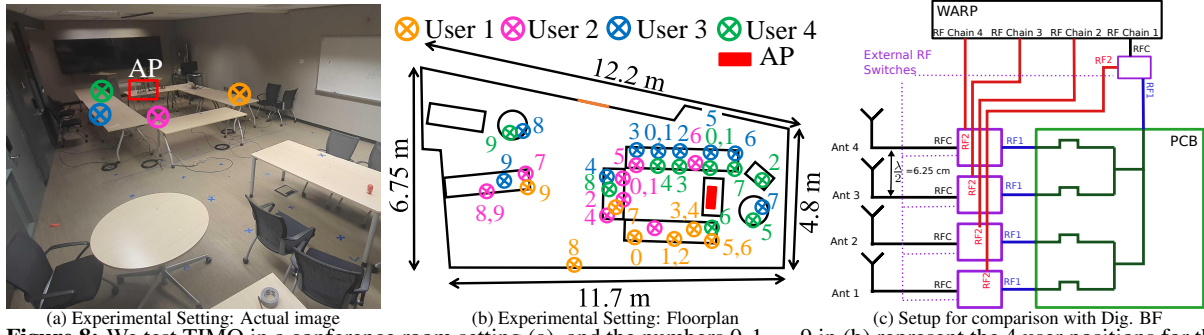


Figure 8: We test TIMO in a conference room setting (a), and the numbers 0, 1, ..., 9 in (b) represent the 4 user positions for the 10 configurations where we test TIMO and other baselines, (c) shows the setup for faithful comparisons with digital beamforming

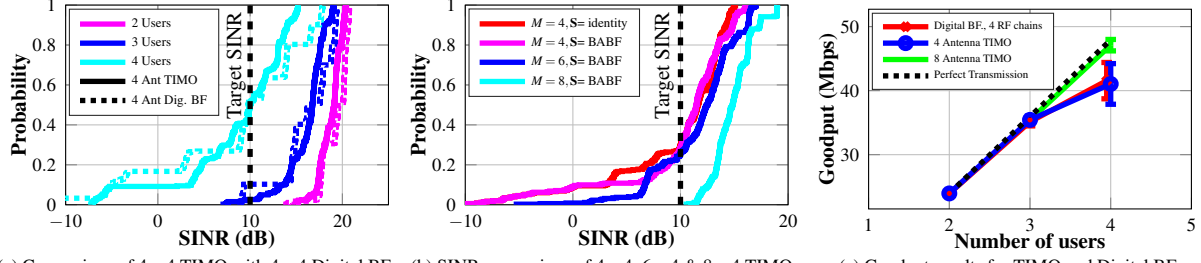
us to use the same antennas for capturing the received samples from WARP with both 4 virtual RF chains created by TIMO's approach of having an overlocked single RF chain, and 4 physical RF chains with a slower ADC on each chain.

For this experiment, we use only a 4 antenna TIMO configuration, and since we oversample 4 times to sample the transmitted 10 MHz users' signals at 40 MHz sampling bandwidth of WARP (as discussed in 4), we have 4 virtual RF chains. Thus, as number of antennas are same as number of virtual RF chains, we can set the switching matrix \mathbf{S} as identity, to configure TIMO to obtain per antenna channel estimates at each of the virtual RF chains and thus emulate what digital beamforming would do. Thus, we expect to see similar performance metrics as compared to digital beamforming. Both SINR and the obtained goodput performances of both the methods indeed turn out to be very similar (Fig. 9a, Fig. 9c). The SINR here is computed from the EVM metric of the received constellation after digital combining is done, as the noise would be coming from the residual interference and noise. Goodput is measured by mapping the received constellation back to bits, passing through viterbi decoder corresponding to the 0.5 rate convolutional code, and then measuring the number of bit errors. We perform this experiment to collect 30 packets at each of the 10 locations of 4 users in the conference room floor-

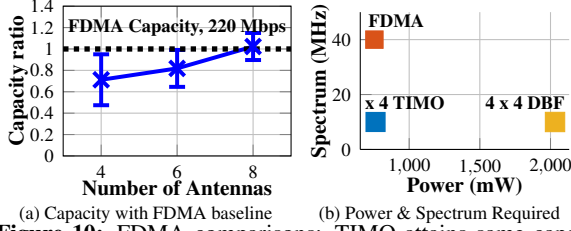
plan, which gives 300 sample SINRs and goodput metrics for these plots. The CDFs are plotted with these sample data points, and we can clearly see the performance for both the methods to be very similar (within ± 0.5 dB for median error), and the average goodput observed across these 300 total packets is almost indistinguishable with each other.

However, one thing can be clearly seen is that as the number of users increase from 2 to 4, the performance of both the two approaches deteriorate, and with 4 users, for almost 40% of the packets, the SINR is lesser than 10 dB (Fig. 9a), for which our chosen MCS of QAM16 constellation with 0.5 rate convolutional code doesn't perform well, leading to bit errors as high as 10-15%, and thus leading to a reduction in throughput (Fig. 9c). This result is consistent with many of the research papers [47, 48], which all agree on the fact that serving as many users as number of RF chains is not a very robust operating points for digital beamformers. Infact, this limitation of not being able to deliver K multiplexing gain while using K RF chains has been one of the biggest setbacks for mu-MIMO and thus it has not found wide adoptability.

Hardening of multiplexing gains by utilizing 8 antennas to serve 4 users: We utilize the 8 antenna version of our TIMO architecture, as shown in Fig. 6 to implement BABF algorithm in order to support 4 users reliably. Note that we do not increase our oversampling fac-



(a) Comparison of 4×4 TIMO with 4×4 Digital BF. (b) SINR comparison of 4×4 , 6×4 & 8×4 TIMO (c) Goodput results for TIMO and Digital BF
Figure 9: Experiment CDFs for SINR plotted across multiple packets collected for multiple user locations in the conference room setting, and Average Goodput with errorbars representing std. deviation across multiple packets. We can see that with 8×4 TIMO, we always meet the target SINR which allows robust goodput performance for all users



(a) Capacity with FDMA baseline (b) Power & Spectrum Required
Figure 10: FDMA comparisons: TIMO attains same capacity with SINR performance similar to user SNR's in different frequency bands for FDMA. We also compare the power and spectrum required by different approaches

tor, and just attach more switched antennas for this experiment. Thus, we do not expect to see an improvement in the multiplexing gain as such, but the multiplexing gain of 4 should become robust and this is also referred to as ‘hardening’ of the multiplexing gain.

As we have already shown the equivalence between 4 antenna TIMO with S as identity matrix and 4 antenna digital beamforming, we do not collect data again with the digital beamforming setup, and just utilize a single RF chain on WARP connected to the output coming from our TIMO PCB after combining across the 8 switched antennas. We can electronically turn off antennas in our PCB to simultaneously collect data from 4, as well as 6 antenna configurations to understand the effect of increasing number of antennas on the system metrics. To choose the switching matrix S , we utilize BABF algorithm and select the maximal set of antennas in-phase for one user at a time, in order to prioritize one user per virtual RF chain. This also allows the equivalent 4×4 digital channel to be orthogonal and full rank, such that digital beamforming can now perform to its limit.

The SINR and goodput results are shown in Fig. 9b, and Fig. 9c. We indeed observe the hardening effect as we increase the antennas to 8, since the SINR always exceeds 10 dB, which makes the system an excellent operating point for QAM-16 constellation, allowing goodput to be close to what is expected from a robust multi-user transmission scheme. We observe more than 10 dB increase in the 90-th percentile SINR, as compared to 4 antenna TIMO with identity S , which has been shown earlier to work exactly same as a 4 antenna digital beam-

former. Similar to how it is for analog beamforming, we also see that BABF algorithm’s performance increases as number of antennas increase, which is because more antennas would allow for a higher constructive combining gain. Thus, for $M = 4$, the performance with and without BABF is almost similar, but increases tremendously as M increases to 8. It is indeed impressive to see how TIMO was able to harden the multiplexing gains for 4 users without actually increasing the number of virtual RF chains just by utilizing more switched antennas, which bear a very minimal extra power and implementation cost.

Comparison with interference-free FDMA baseline:

Since TIMO utilizes 4 times higher sampling bandwidth as the user’s transmitting bandwidth, it is only natural to compare the same with an equivalent frequency based multiplexing (FDMA) system. For the FDMA baseline, the users will occupy 4 different 10 MHz bands, and the WARP would sample this aggregate 40 MHz bandwidth in order to serve these 4 users. In contrast, for TIMO, the 4 users will be occupying the same 10 MHz band, and the WARP receiver would sample a higher sampling bandwidth 40 MHz, in order to create the 4 virtual RF chains required to multiplex the 4 users signals. Thus, TIMO utilizes 4 times lesser spectrum resources, while utilizing the same sampling bandwidth as FDMA.

However the challenge in TIMO’s comparison to FDMA is if TIMO can cancel the interference effectively in order to be comparable to FDMA’s spectrum heavy but interference free multiplexing. For this reason, TIMO is equipped multiple switched antennas, whereas FDMA can work with just a single antenna. Again, here we see benefits of utilizing more number of antennas than number of users, as we can see from Fig. 10a, increasing to 8 antennas gives system capacity on par with FDMA. In fact, we observe sometimes that 8 antenna TIMO even outperforms the FDMA baseline, as TIMO is able to tap into the constructive combining gains from multiple in-phase antennas being on at the same time. For this result, we compute the capacity by calculating SINR from the LTS preambles after combining in order to characterize the system capacity instead of calculating the SINR from

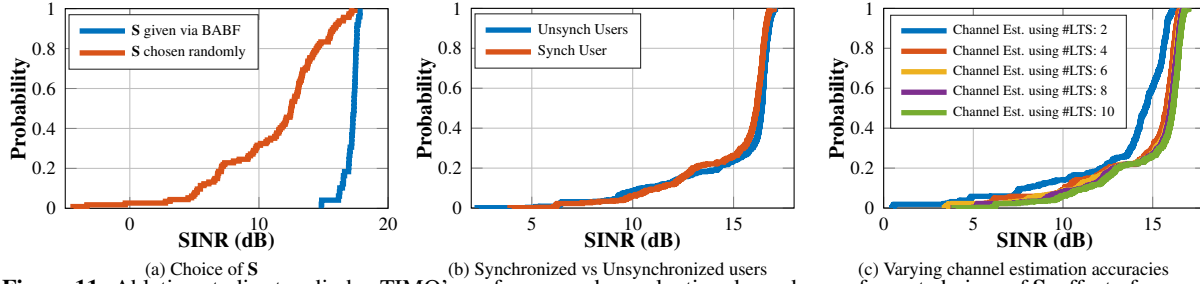


Figure 11: Ablation studies to adjudge TIMO’s performance, by evaluating dependence of smart choices of \mathbf{S} , effect of unsynchronized versus tightly synchronized users, and dependence of cancellation on the channel estimation accuracies

the EVM of our chosen QAM-16 constellation.

Spectrum saving and Power saving with TIMO: So far, we have seen that TIMO serves four users utilizing 4x lower spectrum than equivalent FDMA system and 4x lower RF-chains than equivalent MIMO system while performing similar to FDMA and MIMO systems. Here we explain the implication of saving these spectrum and hardware resources on modern communication systems as shown in Figure 10b. First, TIMO is spectrally efficient as it utilizes only 10 MHz bandwidth to serve 4 users while an equivalent FDMA system requires a large 40 MHz spectrum. Thus, TIMO achieves 4x higher spectral efficiency than FDMA.

The second implication is that TIMO is power efficient as it saves the number of RF chains by a factor of four compared to a MIMO system. To concrete our claims, we profile the power consumption of ADC and downconversion chain with our WARPv3 implementation. WARPv3’s RF transceiver MAX2829 [54] requires 1632 mW (4×408 mW) power when operating in MIMO mode, while only 354 mW for TIMO operating in the SISO mode. ADC power varies linearly with the sampling frequency [9], and so the power consumption of 4 ADCs is similar to that of one ADC with 4x higher sampling (which evaluates to 400 mW for both MIMO and TIMO systems for the AD9963 ADC [55] used in WARPv3). Finally, TIMO uses a network of switches which has negligible power consumption. The HMC197BE switches used in TIMO design require 0.001 mW of static power, and even including the active power they draw from the MHz clock sources, it is less than 1 mW. Therefore, total power consumption of TIMO is 762 mW ($354 + 400 + 8$ mW) which is 3x lower than MIMO ($1632 + 400 = 2032$ MW), and almost the same as single antenna FDMA, which would be 754 mW ($354 + 400$ mW). *In summary, TIMO makes the best of both worlds by being as power-efficient as FDMA systems and as spectrum efficient as MIMO systems. This leads to a scalable mu-MIMO design that can multiplex an order of magnitude higher users simultaneously.*

Ablation studies: Finally, to conclude TIMO’s evaluation we show how factors like choice of the matrix \mathbf{S} , having users unsynchronized and channel estimation

accuracy play a factor into TIMO’s approach. For all these results we fix a 4 user configuration in the conference room setting and collect multiple packets by varying these parameters to carefully understand the effects.

Recall that via BABF, we use the switches to increase the signal power of one user for each virtual RF chain, so that we get as close to orthogonal 4×4 equivalent channel so that multiplexing gain can harden. To evaluate the effectiveness of our algorithm, we choose 100 random choices of \mathbf{S} , and collect 10 packets with each choice, and repeat the same with 100 packets collected by choosing \mathbf{S} given by BABF algorithm to choose in-phase switches for one user per virtual RF chain. We plot the CDF in Fig. 11a, and observe that the intelligent way of choosing \mathbf{S} always outperforms a randomly chosen \mathbf{S} , thus showing the effectiveness of our BABF algorithm.

We also show robustness to transmitters being unsynchronized with each other in Fig. 11b. Note that for none of our experiments, receiver was never synchronized with the transmitters. For this experiment, the transmitters were first synchronized to each other by utilizing same reference clock and start time, and thus all the transmitters have same CFO and tightly synchronized sampling times. In the unsynchronized experiment only the start time was shared across the nodes, and each node had a different clock, leading to different CFOs for each user. As clearly seen from Fig. 11b, we get almost the same performance when the transmitters are synchronised with each other as compared to when they are unsynchronized. Infact, we get minimally higher SINR with unsynchronized since due to sampling offsets, the unsynchronized transmissions often end up having some samples to be interference free, whereas for the synchronized transmissions, all the user’s signals interfere all the times, hence being a more stringent evaluation. These results prove that since TIMO does a spatial operation it is robust to any kind-of CFO effects and it does not matter if things are not synchronized to get similar performance.

Finally, since TIMO utilized the channel estimates to compute \mathbf{S} and the digital precoding matrix \mathbf{V} , the interference cancellation performance also depends on the accuracy of channel estimates procured. We can always average the channel across multiple LTS’s to get a higher

channel estimation accuracy. Thus, we repeat the experiment with more number of LTS's than the prescribed 2 LTS's as per 802.11 protocol, and observe that we get only about 1.5 dB difference in median performance as the number of LTS's increase to 10, which shows that TIMO's algorithms can work without imposing a high cost of channel estimation latency.

TIMO can also generalize to perform spatio-temporal combining if multiple RF chains are available. Basically having a second RF chain allows TIMO to create $2t$ number of total RF chains, as for each RF chain we can construct t virtual time separated RF chains. This allows for a multiplicative increase in the number of users to be supported. Here, we would like to point that TIMO is different from the prior work in hybrid beamforming which is bottlenecked by number of RF chains. By utilizing artificial faded created in the wireless channel due to fast switching, we can scale well with number of users.

6 Discussion and Future Work

Scaling to higher number of antennas and users: TIMO is a scalable architecture for multi-user system that utilizes a switched antenna array and a single down-conversion chain to multiplex many users. The TIMO architecture naturally scales to a large number of users with even higher power savings. To demonstrate these gains, we calculate the power requirement for TIMO for up to 50 users and compare them against other digital or hybrid architectures. Figure 12 shows that the power scales linearly with the number of users for all the systems. In Fig. 12, we consider a passive mixer with insertion loss of 7dB and drawing LO power of 10 dBm, and phase shifters with insertion loss of 10dB, and finally switches with insertion loss of 1 dB and clock power consumption of 1 dBm. To offset the insertion losses, we consider a LNA with FoM 6.5 mW^{-1} and noise figure 3dB [9]. The ADCs sample at 20mW per Msps, and the per user bandwidth is assumed to be 20 MHz.

We observe that TIMO power scales slowly (smaller slope value) with users. With 40 users, hybrid beamforming with 2K antennas would require $2\times$ higher power compared to TIMO. Moreover, both versions of TIMO with K or 2K antennas require almost similar power to serve K users, which comes mainly due to the high-sampling ADC used in TIMO. In this way, TIMO is better scalable to multiple users than traditional multi-user systems. We keep the system prototype for $K > 4$ users/antennas as our future work.

Scaling to wider bandwidths: In this paper, we have evaluated TIMO for a maximum of 4 users having a bandwidth of 10 MHz. This was mainly limited due to the system constraints posed by our choice of WARPv3 as a receiver SDR which has a sampling rate of 40 MHz. However, TIMO architecture can easily scale to wider-bandwidth. The two key component of TIMO archi-

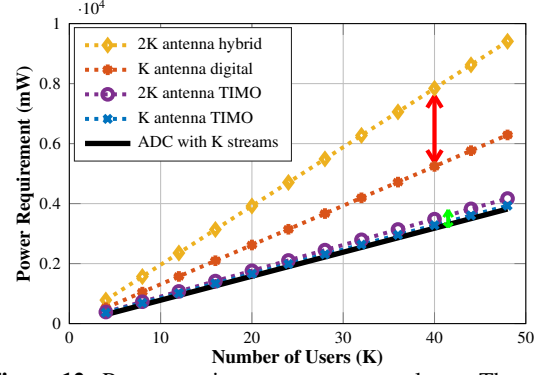


Figure 12: Power requirements as users scale up: The red arrow shows the extra power consumed by LNA required to offset the insertion losses with phase shifters, in addition to requiring K RF chains to serve K users reliably with $2K \times K$ hybrid analog network of phase shifters. In contrast, TIMO's architecture hybridizes with minimal extra cost (green arrow) since switches have < 1 dB insertion loss.

ture are switches and ADCs. There are easily available ADCs now capable of 1 GHz sampling bandwidth [56, 57], which can easily support 50 virtual chain at 20 MHz sampling, typical bandwidth for most sub-6 GHz communication. The improvement in ADC technology is to enable mmWave frequencies, which is rarely deployed. Today, more than 95% devices operate in sub-6 band [58], and TIMO architecture gives an application where these ADCs can be developed to serve more users in sub-6 and alleviate the spectrum crunch we have today with sub-6 devices.

Next, The needs for fast switches, as TIMO has these switches at the heart of the architecture, as it is this humble RF switch which implements both digital, and hybrid beamformers with TIMO architecture. Photonic RF switches under development in research labs offer pico-second rise time [59–61], alongwith a few commercially available switches offering sub-ns rise times [62], easily can enable 1 GHz switching speed. TIMO's architecture can lead to these switches being common in the circuits marketplace. Thus, integration with high sample rate ADCs and pico-second fast RF switches would form a future direction for TIMO architecture

Utilizing TIMO in tandem with multiple physical RF Chains: In this paper, we have tested TIMO architecture with just a single RF chain. However, if we have multiple RF chains, all capable of clocking at higher sampling rates, TIMO can create a multiple set of virtual RF chains from each of these physical RF chains. Thus, TIMO's time combining can be viewed as an alternate to traditional space combining method. By utilizing space-time combining we can increase the number of users supported by both TIMO's architecture of single RF chains and traditional digital beamforming's slower clocking multiple physical RF chains. Demonstrating this is an immediate future direction for TIMO.

References

- [1] Daniel C Araújo, Taras Maksymyuk, André LF de Almeida, Tarcisio Maciel, João CM Mota, and Minho Jo. Massive mimo: survey and future research topics. *Iet Communications*, 10(15):1938–1946, 2016.
- [2] Jakob Hoydis, Stephan Ten Brink, and Mérouane Debbah. Massive mimo in the ul/dl of cellular networks: How many antennas do we need? *IEEE Journal on selected Areas in Communications*, 31(2):160–171, 2013.
- [3] Lingjia Liu, Runhua Chen, Stefan Geirhofer, Krishna Sayana, Zhihua Shi, and Yongxing Zhou. Downlink mimo in lte-advanced: Su-mimo vs. mu-mimo. *IEEE Communications Magazine*, 50(2):140–147, 2012.
- [4] Eduardo Castaneda, Adao Silva, Atilio Gameiro, and Marios Kountouris. An overview on resource allocation techniques for multi-user mimo systems. *IEEE Communications Surveys & Tutorials*, 19(1):239–284, 2016.
- [5] Jian Ding, Rahman Doost-Mohammady, Anuj Kalia, and Lin Zhong. Agora: Real-time massive mimo baseband processing in software. In *Proceedings of the 16th International Conference on emerging Networking EXperiments and Technologies*, pages 232–244, 2020.
- [6] Susnata Mondal, Rahul Singh, Ahmed I Hussein, and Jeyanandh Paramesh. A 25–30 GHz fully-connected hybrid beamforming receiver for MIMO communication. *IEEE Journal of Solid-State Circuits*, 53(5):1275–1287, 2018.
- [7] Susnata Mondal, Rahul Singh, Ahmed I Hussein, and Jeyanandh Paramesh. A 25–30 GHz 8-antenna 2-stream hybrid beamforming receiver for MIMO communication. In *2017 IEEE Radio Frequency Integrated Circuits Symposium (RFIC)*, pages 112–115. IEEE, 2017.
- [8] Susnata Mondal, Rahul Singh, and Jeyanandh Paramesh. 21.3 a reconfigurable bidirectional 28/37/39GHz front-end supporting MIMO-TDD, carrier aggregation TDD and FDD/Full-duplex with self-interference cancellation in digital and fully connected hybrid beamformers. In *2019 IEEE International Solid-State Circuits Conference (ISSCC)*, pages 348–350. IEEE, 2019.
- [9] C Nicolas Barati, Sourjya Dutta, Sundeep Rangan, and Ashutosh Sabharwal. Energy and latency of beamforming architectures for initial access in mmwave wireless networks. *Journal of the Indian Institute of Science*, 100(2):281–302, 2020.
- [10] Hong-Teuk Kim, Byoung-Sun Park, Seong-Sik Song, Tak-Su Moon, So-Hyeong Kim, Jong-Moon Kim, Ji-Young Chang, and Yo-Chul Ho. A 28-GHz cmos direct conversion transceiver with packaged 2*4 antenna array for 5G cellular system. *IEEE Journal of Solid-State Circuits*, 53(5):1245–1259, 2018.
- [11] Thomas Kühne, Piotr Gawłowicz, Anatolij Zubow, Falko Dressler, and Giuseppe Caire. Bringing hybrid analog-digital beamforming to commercial MU-MIMO wifi networks. In *Proceedings of the 26th Annual International Conference on Mobile Computing and Networking*, pages 1–3, 2020.
- [12] Yasaman Ghasempour, Muhammad K Haider, Carlos Cordeiro, Dimitrios Koutsonikolas, and Edward Knightly. Multi-stream beam-training for mmWave MIMO networks. In *Proceedings of the 24th Annual International Conference on Mobile Computing and Networking*, pages 225–239, 2018.
- [13] Xiufeng Xie, Eugene Chai, Xinyu Zhang, Karthikeyan Sundaresan, Amir Khojastepour, and Sampath Rangarajan. Hekaton: Efficient and practical large-scale MIMO. In *Proceedings of the 21st Annual International Conference on Mobile Computing and Networking*, pages 304–316, 2015.
- [14] Yongce Chen, Yan Huang, Chengzhang Li, Y Thomas Hou, and Wenjing Lou. Turbo-HB: A novel design and implementation to achieve ultra-fast hybrid beamforming. In *IEEE INFOCOM 2020-IEEE Conference on Computer Communications*, pages 1489–1498. IEEE, 2020.
- [15] Didi Zhang, Yafeng Wang, Xuehua Li, and Wei Xiang. Hybridly connected structure for hybrid beamforming in mmWave massive MIMO systems. *IEEE Transactions on Communications*, 66(2):662–674, 2017.
- [16] Xianghao Yu, Juei-Chin Shen, Jun Zhang, and Khaled B Letaief. Alternating minimization algorithms for hybrid precoding in millimeter wave MIMO systems. *IEEE Journal of Selected Topics in Signal Processing*, 10(3):485–500, 2016.
- [17] Tatsunori Obara, Tatsuki Okuyama, Yuuichi Aoki, Satoshi Suyama, Jaekon Lee, and Yukihiko Okumura. Indoor and outdoor experimental trials in

- 28-GHz band for 5G wireless communication systems. In *2015 IEEE 26th Annual International Symposium on Personal, Indoor, and Mobile Radio Communications (PIMRC)*, pages 846–850. IEEE, 2015.
- [18] Zhe Chen, Xu Zhang, Sulei Wang, Yuedong Xu, Jie Xiong, and Xin Wang. BUSH: empowering large-scale MU-MIMO in WLANs with hybrid beam-forming. In *IEEE INFOCOM 2017-IEEE Conference on Computer Communications*, pages 1–9. IEEE, 2017.
- [19] Fred Tzeng, Amin Jahanian, Deyi Pi, and Payam Heydari. A cmos code-modulated path-sharing multi-antenna receiver front-end. *IEEE journal of solid-state circuits*, 44(5):1321–1335, 2009.
- [20] Manoj Johnson, Armagan Dascurcu, Kai Zhan, Arman Galioglu, Naresh Kumar Adepu, Sanket Jain, Harish Krishnaswamy, and Arun S Natarajan. Code-domain multiplexing for shared IF/LO interfaces in millimeter-wave MIMO arrays. *IEEE Journal of Solid-State Circuits*, 55(5):1270–1281, 2020.
- [21] Robin Garg, Gaurav Sharma, Ali Binaie, Sanket Jain, Sohail Ahasan, Armagan Dascurcu, Harish Krishnaswamy, and Arun S Natarajan. A 28-GHz beam-space MIMO RX with spatial filtering and frequency-division multiplexing-based single-wire IF interface. *IEEE Journal of Solid-State Circuits*, 2020.
- [22] Sohrab Madani, Suraj Jog, Jesús Omar Lacruz, Joerg Widmer, and Haitham Hassanieh. Practical null steering in millimeter wave networks. In *NSDI*, pages 903–921, 2021.
- [23] Osama N Alrabadi, Chamath Divarathne, Philippos Tragas, Antonis Kalis, Nicola Marchetti, Constantinos B Papadias, and Ramjee Prasad. Spatial multiplexing with a single radio: Proof-of-concept experiments in an indoor environment with a 2.6-GHz prototype. *IEEE Communications Letters*, 15(2):178–180, 2010.
- [24] Bo Han, Vlasios I Barousis, Constantinos B Papadias, Antonis Kalis, and Ramjee Prasad. MIMO over ESPAR with 16-QAM modulation. *IEEE Wireless Communications Letters*, 2(6):687–690, 2013.
- [25] Heung-Gyoon Ryu and Bong-Jun Kim. Beam space MIMO-OFDM system based on ESPAR antenna. In *2015 International Workshop on Antenna Technology (iWAT)*, pages 168–171. IEEE, 2015.
- [26] Yafei Hou, Rian Ferdian, Satoshi Denno, and Minoru Okada. Low-complexity implementation of channel estimation for ESPAR-OFDM receiver. *IEEE Transactions on Broadcasting*, 67(1):238–252, 2020.
- [27] Illsoo Sohn and Donghyuk Gwak. Single-RF MIMO-OFDM system with beam switching antenna. *EURASIP Journal on Wireless Communications and Networking*, 2016(1):1–14, 2016.
- [28] Junho Lee, Ju Yong Lee, and Yong H Lee. Spatial multiplexing of OFDM signals with QPSK modulation over ESPAR. *IEEE Transactions on Vehicular Technology*, 66(6):4914–4923, 2016.
- [29] Zixiang Han, Yujie Zhang, Shanpu Shen, Yue Li, Chi-Yuk Chiu, and Ross Murch. Characteristic mode analysis of ESPAR for single-RF MIMO systems. *IEEE Transactions on Wireless Communications*, 20(4):2353–2367, 2020.
- [30] Jung-Nam Lee, Yong-Ho Lee, Kwang-Chun Lee, and Tae Joong Kim. $\lambda/64$ -spaced compact ESPAR antenna via analog RF switches for a single RF chain MIMO system. *ETRI Journal*, 41(4):536–548, 2019.
- [31] Gweondo Jo, Hyoung-Oh Bae, Donghyuk Gwak, and Jung-Hoon Oh. Demodulation of 4×4 MIMO signal using single RF. In *2016 18th International Conference on Advanced Communication Technology (ICACT)*, pages 390–393. IEEE, 2016.
- [32] Grzegorz Bogdan, Konrad Godziszewski, and Yevhen Yashchyshyn. MIMO receiver with reduced number of RF chains based on 4D array and software defined radio. In *2019 27th European Signal Processing Conference (EUSIPCO)*, pages 1–5. IEEE, 2019.
- [33] Grzegorz Bogdan, Konrad Godziszewski, Yevhen Yashchyshyn, Cheol Ho Kim, and Seok-Bong Hyun. Time-modulated antenna array for real-time adaptation in wideband wireless systems—part i: Design and characterization. *IEEE Transactions on Antennas and Propagation*, 68(10):6964–6972, 2019.
- [34] Grzegorz Bogdan, Konrad Godziszewski, and Yevhen Yashchyshyn. Time-modulated antenna array for real-time adaptation in wideband wireless systems—part ii: Adaptation study. *IEEE Transactions on Antennas and Propagation*, 68(10):6973–6981, 2020.

- [35] José P González-Coma and Luis Castedo. Wide-band hybrid precoding using time modulated arrays. *IEEE Access*, 8:144638–144653, 2020.
- [36] Grzegorz Bogdan, Konrad Godziszewski, and Yevhen Yashchyshyn. Time-modulated antenna array with beam-steering for low-power wide-area network receivers. *IEEE Antennas and Wireless Propagation Letters*, 19(11):1876–1880, 2020.
- [37] Wen-Qin Wang, Hing Cheung So, and Alfonso Farina. An overview on time/frequency modulated array processing. *IEEE Journal of Selected Topics in Signal Processing*, 11(2):228–246, 2016.
- [38] José P González-Coma, Roberto Maneiro-Catoira, and Luis Castedo. Hybrid precoding with time-modulated arrays for mmwave MIMO systems. *IEEE Access*, 6:59422–59437, 2018.
- [39] Avishek Chakraborty, Gopi Ram, and Durbadal Mandal. Time-modulated multibeam steered antenna array synthesis with optimally designed switching sequence. *International Journal of Communication Systems*, 34(9):e4828, 2021.
- [40] Chong He, Xianling Liang, Bin Zhou, Junping Geng, and Ronghong Jin. Space-division multiple access based on time-modulated array. *IEEE Antennas and Wireless Propagation Letters*, 14:610–613, 2014.
- [41] Roberto Maneiro-Catoira, Julio Brégains, José A García-Naya, and Luis Castedo. Time modulated arrays: From their origin to their utilization in wireless communication systems. *Sensors*, 17(3):590, 2017.
- [42] Grzegorz Bogdan, Miłosz Jarzynka, and Yevhen Yashchyshyn. Experimental study of signal reception by means of time-modulated antenna array. In *2016 21st International Conference on Microwave, Radar and Wireless Communications (MIKON)*, pages 1–4. IEEE, 2016.
- [43] Shyamnath Gollakota, Samuel David Perli, and Dina Katabi. Interference alignment and cancellation. In *Proceedings of the ACM SIGCOMM 2009 conference on Data communication*, pages 159–170, 2009.
- [44] Fadel Adib, Swarun Kumar, Omid Aryan, Shyamnath Gollakota, and Dina Katabi. Interference alignment by motion. In *Proceedings of the 19th annual international conference on Mobile computing & networking*, pages 279–290, 2013.
- [45] Adriana B Flores, Sadia Quadri, and Edward W Knightly. A scalable multi-user uplink for Wi-Fi. In *13th {USENIX} Symposium on Networked Systems Design and Implementation ({NSDI} 16)*, pages 179–191, 2016.
- [46] Wi-Fi spectrum crunch: How to beat slow speeds in crowded areas. <https://www.makeuseof.com/tag/wi-fi-spectrum-crunch/>.
- [47] Hannaneh Barahouei Pasandi, Tamer Nadeem, and Hadi Amirpour. MuViS: Online MU-MIMO grouping for multi-user applications over commodity WiFi. *arXiv preprint arXiv:2106.15262*, 2021.
- [48] Sanjib Sur, Ioannis Pefkianakis, Xinyu Zhang, and Kyu-Han Kim. Practical MU-MIMO user selection on 802.11 ac commodity networks. In *Proceedings of the 22nd Annual International Conference on Mobile Computing and Networking*, pages 122–134, 2016.
- [49] Shi Su, Wai-Tian Tan, Xiaoqing Zhu, Rob Liston, and Behnaam Aazhang. Data-driven mode and group selection for downlink MU-MIMO with implementation in commodity 802.11 ac network. *IEEE Transactions on Communications*, 69(3):1620–1634, 2021.
- [50] Delayseq. <https://www.mathworks.com/help/phased/ref/delayseq.html>.
- [51] Mattia Rebato, Luca Rose, and Michele Zorzi. Performance assessment of MIMO precoding on realistic mmWave channels. In *2019 IEEE International Conference on Communications Workshops (ICC Workshops)*, pages 1–6. IEEE, 2019.
- [52] HMC197BE. <https://www.analog.com/media/en/technical-documentation/data-sheets/hmc197b.pdf>.
- [53] X410 SDR. <https://www.ettus.com/all-products/usrp-x410/>.
- [54] MAX2829. <https://datasheets.maximintegrated.com/en/ds/MAX2828-MAX2829.pdf>.
- [55] AD9963. <https://www.analog.com/en/products/ad9963.html>.
- [56] ADC captures 1Gbps. <https://www.maximintegrated.com/en/design/technical-documents/app-notes/6/642.html>.
- [57] 1 GHz ADC from TI. <https://www.ti.com/lit/ug/tidubq0/tidubq0.pdf>.

- [58] Number of 4g lte connections worldwide from 2012 to 2020. <https://www.statista.com/statistics/736022/4g-lte-connections-worldwide/>.
- [59] Jia Ge and Mable P Fok. Ultra high-speed radio frequency switch based on photonics. *Scientific reports*, 5(1):1–7, 2015.
- [60] Yiwei Xie, Leimeng Zhuang, Pengcheng Jiao, and Daoxin Dai. Sub-nanosecond-speed frequency-reconfigurable photonic radio frequency switch using a silicon modulator. *Photonics Research*, 8(6):852–857, 2020.
- [61] Hengyun Jiang, Lianshan Yan, Wei Pan, Bing Luo, and Xihua Zou. Ultra-high speed RF filtering switch based on stimulated brillouin scattering. *Optics letters*, 43(2):279–282, 2018.
- [62] Hmmc2027 gaas rf switch. <https://www.acalbfi.com/be/RF-components/Switches/p/DC---26-5-{GHz}-SPDT-Absorptive-GaAs-Switch-IC/0000000JUM>.

7 Appendix

7.1 Algorithm to choose maximal set of antennas in-phase

Algorithm 1 Binarized Analog Beamforming Algorithm (BABF)

```

1:  $\phi = \pi/3$ ;
2: for  $1 \leq i \leq K$  do
3:   for  $1 \leq m \leq M$  do
4:      $\tilde{\mathbf{s}}_{i,m} = [0, 0, \dots, 0]_{1 \times M}$ ;
5:      $\mathbf{g}_{i,m} = \mathbf{H}_i \mathbf{h}_{i,m}^*$ ;
6:      $\theta_{i,m} = \angle \mathbf{g}_{i,m}$ ;
7:      $\tilde{\mathbf{s}}_{i,m}(m) = |\theta_{i,m}| < \phi$ ;
8:      $score_{i,m}$  = Number of elements equal to 1 in  $\tilde{\mathbf{s}}_{i,m}$ ;
9:   end for
10: end for
11:  $\mathbb{S} :=$  Set of all possible permutations of  $score_{i,m}, 1 \leq i \leq K, 1 \leq m \leq M$ 
12:  $l = 1$ ;
13: Select  $score^* \in \mathbb{S}$  that provides the  $l^{\text{th}}$  highest score;
14:  $\mathbf{S} = \mathbf{S}^*$  (corresponding to  $score^*$ );
15: if  $\mathbf{H}(f)\mathbf{S}$  is full rank then
16:    $\mathbf{S}$  is the optimal switch configuration;
17: else
18:    $l = l + 1$ ;
19:   Go to line 13;
20: end if
```
